Front. Chem. China 2010, 5(1): 33–44
DOI 10.1007/s11458-009-0112-x

FEATURE ARTICLE

Semiconducting nanocrystals, conjugated polymers, and conjugated polymer/nanocrystal nanohybrids and their usage in solar cells

Lei ZHAO, Jun WANG and Zhiqun LIN (✉)

Department of Materials Science and Engineering, Iowa State University, Ames, IA 50011, USA

As one of the major renewable energy sources, solar energy has the potential to become an essential component of future global energy production. With the increasing demand in energy, the harvesting of solar energy using inexpensive materials and manufacturing methods has attracted considerable attention. Organic/inorganic (i.e., conjugated polymer/nanocrystal (CP/NC)) nanohybrid solar cell, including both physically mixed CP/NC composites and covalently linked CP-NC nanocomposites, is one of the several most promising alternative, cost-effective concepts for solar-to-electric energy conversion that has been offered to challenge conventional Si solar cells over the past decade. It has low fabrication cost and capability of large-scale production. However, to date, the highest power conversion efficiency (PCE) of organic/inorganic nanohybrid solar cells has been reported to be only 5.5%, which is still lower than the theoretical prediction of more than 10%. Several problems, i. e., microscopic phase separation of semiconducting CPs and NCs, low charge injection, and low carrier collection, have not been well addressed. More research remains to be done to improve the efficiency of CP/NC nanohybrid solar cells. In this review article, the recent advances in solving these problems were discussed. For the CP/NC solar cells prepared by physically mixing electron donating CP and electron accepting NC (i.e., forming CP/NC composites), methods involving the use of solvent mixtures and ligand modification to control the phase separation at the nanoscale are discussed; the implications of intriguing anisotropic NCs as well as their assemblies (i.e., NC arrays) on improving the charge collection are presented. For newly developed CP/NC solar cells prepared by chemically tethering CP chains on the NC surface (i.e., yielding CP-NC nanocomposites, thereby preventing microscopic phase separation of CP and NC and improving their electronic interaction), recent strategies on the synthesis of such nanocomposites and their photovoltaic performance are discussed.

Keywords conjugated polymers, nanocrystals, nanohybrid solar cells

1 Introduction

The economy and environment of our times depend on the access to reliable, clean, abundant, and affordable energy, including hydropower, nuclear, biomass, wind, geothermal, and solar energies. Among these energy sources, solar energy represents an effectively unlimited supply of fuel at no cost, and has fewer issues compared with other sources. The earth receives about 100,000 TW of solar power on its surface, meaning solar energy of one hour can supply humanity's energy needs for a whole year [1]. The calculation performed by the National Renewable Energy Laboratory (NREL) shows that solar panels on all usable residential and commercial roof

Received September 21, 2009; accepted November 11, 2009
E-mail: zqlin@iastate.edu

surfaces could provide the United States with as much electricity per annum as the country used in 2004 [1]. Considering the broad desert areas on the earth, for example, the Sahara Desert, the Gobi Desert in central Asia, the Atacama in Peru, and the Great Basin in the United States, produced solar energy will be far more than enough to be used. Despite its advantages, the electricity generated from solar cells is still limited to a small fraction of our overall energy consumption, primarily due to the high cost of manufacturing and installation of the commercial Si solar cells (power conversion efficiency, PCE = ~15%) [2]. Although the cost per watt of crystalline Si solar cells has significantly dropped over the past decade [3], its current cost is still in the range of $0.25–0.40 per watt [1], making it less competitive without the benefit of government subsidies than conventional electricity grids. The second generation solar cells, based on polycrystalline semiconductor thin films, can bring down the price dramatically. However, they still suffer from low efficiency and not being practically viable [4]. With recent advances in nanotechnology, especially in the area of synthesis [5–9] and assembly [10–15] of nanocrystals (NCs), the third generation solar cells based on organic/inorganic nanohybrids has received considerable attention [16,17]. The solar cells of this kind are believed to be able to provide electricity at extremely low cost if reasonable PCE ($>10\%$) and lifetime (>10 y) can be attained on a large scale in the near future [16].

The organic/inorganic nanohybrid solar cells consist of interpenetrating phases of semiconducting conjugated polymers (CPs) and NCs as the active components. The p-type CPs and n-type inorganic NCs are selected as the electron donor and acceptor, respectively. Upon the absorption of photons, electrons of CP are excited from the high occupied molecular orbital (HOMO) to the low unoccupied molecular orbital (LUMO) by harvesting a photon with energies greater than the band gap, thereby generating an exciton (i.e., electron-hole pair). Subsequently, the electrons injection (i.e., charge transfer) from CP into NC is energetically favored when the electronic structures of CP and NC are well coupled, which means $E_{\mathrm{NP}}^{\mathrm{A}} - E_{\mathrm{CP}}^{\mathrm{A}} > U_{\mathrm{CP}} - V_{\mathrm{chargetransfer}}^{2}$, where $E_{\mathrm{NP}}^{\mathrm{A}}$ and $E_{\mathrm{CP}}^{\mathrm{A}}$ are electron affinities of NCs and CPs, respectively, U_{CP} is the Coulombic binding energy of the singlet exciton on the polymer, and $V_{\mathrm{chargetransfer}}$ is the Coulombic energy associated with attraction between electron and hole in the final charge-separated state. In general, $V_{\mathrm{chargetransfer}}$ is much smaller than U_{CP} and can be ignored due to the increased average electron-hole separation in the charge-separated state [18]. In most CPs, excitons have a binding energy of only a fraction of an eV [19,20]. The difference in electron affinities of CP and NC is typically around several eV [2], and hence provides enough driving force for the exciton dissociation at the CP/NC interface. In general, the recombination of electrons and holes occurs in the form of the radiative and nonradiative decays of excitons during the diffusion and dissociation process. Thus, the exciton diffusion length, defined as the average length over which the exciton can diffuse within the polymer before recombination, should be large enough for efficient charge generation. And charge separation process must also be fast enough compared to the radiative and nonradiative decays of the singlet exciton at the CP/NC interface, which typically occur on a time scale of 10–100 picoseconds [2]. After dissociation, the charges (i.e., electrons and holes) migrate to their respective electrodes under an internal electric field due to the difference in their Fermi levels, thereby generating the photocurrent for external loadings.

The performance of the resulting solar cells is dictated by several factors, including the light absorption efficiency, exciton diffusion efficiency, exciton dissociation efficiency, carrier transport efficiency, and charge collection efficiency at electrodes. More detailed information in this aspect can be found in some review articles [2]. In this review article, we present the most recent progress on nanohybrid materials used in solar cells. We first introduce the basic optoelectronic properties of NCs and CPs, then covered the recent advances in the CP/NC nanohybrid solar cells, including both the preparation by physically mixing CP and NC and the chemical integration of CP with NC.

2 Inorganic nanocrystals

A variety of semiconducting nanocrystals (NCs; e.g., CdS, CdSe, and CdTe) have been used in the nanohybrid solar cells. They can be readily synthesized by different methods, including the colloidal method [21–23], the solvent thermal growth [24–27], the vapor-liquid-solid growth [28–31], etc. The NCs widely utilized in nanohybrid solar cells are commonly synthesized using the colloidal method, where a layer of organic molecules are capped on the surface of these colloidal NCs and called ligands or surfactants. This method is very flexible and can be performed in both organic solvent [32,33] and aqueous environment [34,35] at high temperature [32,33] or room temperature [36,37]. A detailed review on this method can be found in literature [5,38]. Because no high-temperature and high-vacuum vapor-deposition are required as in the fabrication of crystalline Si solar cells, the wet-chemical method greatly reduces the cost of solar cells, making it very competitive in the solar cell market. Another notable advantage of this method is that the growth process of NCs can be readily manipulated, leading to well controlled size distribution and shapes of NCs. Both size and shape of

NCs are critical to the performance of NCs in solar cells. To date, various shapes of NCs, including dots, rods, tetrapods, wires, and highly branched structures, have been synthesized with controlled size. In general, these nanostructures can be divided into two categories: isotropic NCs (i.e., quantum dots (QDs)) and anisotropic NCs (other than QDs). The optical properties of NCs will be discussed in the following.

The excitons in NC can be viewed as electrons trapped in a finite potential well, leading to discrete allowed energy levels for electrons. These allowed energy levels produce band gaps where no electrons are allowed. Upon the absorption of photons, an electron is excited from a low energy state to an unoccupied, high energy state by absorbing the exact amount of energy from the photon that matches the band gap. This band gap is highly dependent on the size of NCs. By assuming the energy band parabolic near the band gap, theoretical calculation shows that the size dependent shift in the exciton energy with respect to the band gap in the bulk can be given as [39]:

$$\Delta E = \frac{h^2\pi^2}{2R^2}\left(\frac{1}{m_e}+\frac{1}{m_h}\right)-\frac{1.768e^2}{\varepsilon R}-0.248E^*_{R_y}$$

where R is the NC radius, $E^*_{R_y}$ is the effective Rydberg energy, m_e and m_h are effective mass of electron and holes, respectively, and ε is the dielectric constant. Thus the band gap can be systematically tuned by changing the NC size. Figure 1 illustrates the highly emissive nature of CdSe QDs as a function of particle size. The trioctylphosphine oxide (TOPO) functionalized CdSe QDs dissolved in chloroform were excited with a UV radiation. The size of QDs can be well controlled by altering the growth time of reagents [40,41]. When the band gap is adjusted in the range between 1.77 and 3.1 eV (corresponding to the wavelength of 700 and 400 nm, respectively), the photons are absorbed in the visible region. In current research, cadmium based NCs are used for solar cells because their band gaps span the visible region, from UV to the near infrared, and hence facilitate the absorption of sunlight.

Moreover, NCs generate multiple excitons from a single photon of sufficient energy (e.g., multiple excitons per photon formed in PbSe, PbS, PbTe, and CdSe QDs) [42–52] thereby increasing the photocurrent to enhance conversion efficiency and greatly advance solar fuel producing technologies [44]. Although the occurrence of carrier multiplication has been under debate [53–55], the carrier multiplication efficiency, $\eta_{CM} = 1.7$ was observed for excitation near 4.8 times the band gap for PbSe NCs [53]. As discussed above, when the incident energy is greater than the band gap, electrons at the low energy absorb the energy of the photon, which is equivalent to the band gap, and jump to the high energy level. However, if the incident energy is twice the band gap, another electron could, theoretically, absorb the energy and is excited to a higher energy level. As a result, one incident photon can produce multiple electron-hole pairs, which is called MEG (Figure 2) [42–45,53,56]. Possible reasons explaining the MEG capabilities of QDs include their carrier confinement and increased electron-hole Coulomb interaction [44,45]. In bulk semiconductors, MEG is not typically observed due to a larger number of allowed energy levels and long-range lattice order. In a bulk semiconductor, when an electron is excited from the valence band, the electron may not just simply jump to the next energy level. Instead, the electron may jump to the energy level two or more levels away from the ground level. Subsequently, by dissipating energy through heat to the lattice, the electron drops to the energy level immediately above the ground level, i.e., the conduction band. In QDs, however, there is no long-range order of lattices since the size of QDs is on the order of a few nanometers, and excitons are spatially confined in three dimensions.

Figure 1 Emission of CdSe QDs of different size. The TOPO functionalized CdSe QDs dissolved in chloroform were excited with an UV radiation. Images were obtained in the Lin research group at the Department of Materials Science and Engineering at the Iowa State University.

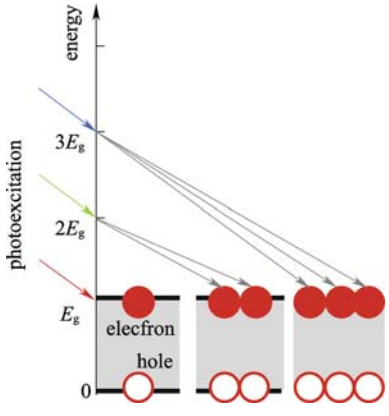

Figure 2 Schematic illustration of multiple exciton generation. Photons with energies E_g, $2E_g$, and $3E_g$ produce one, two, and three excitons, respectively. Figure was reprinted with permission from Ref. [44].

The ability to manipulate the shape of NCs has led to anisotropic NCs (e.g., quantum rods (QRs) with diameters ranging from 2 to 10 nm and lengths ranging from 5 to 100 nm) [34,57]. Because of their intrinsic structural anisotropy, these NCs possess many unique properties that make them potentially better candidates for photovoltaic cells and biomedical applications than QDs. Photovoltaic cells made of anisotropic NCs and CPs show an improved optical absorption in the red and near-infrared ranges originating from the anisotropic NCs [58]; they possess higher absorption coefficient. Moreover, the long axis of the anisotropic NCs provides continuous paths for transporting electrons [59]. The anisotropic NCs possess the polarized emission and their Stokes shift is dependent upon their aspect ratio [34,57,60]. It was found that the external quantum efficiency increased by increasing the aspect ratio of CdSe NCs, i.e., from dots to long rods, (Figure 3) [21]. The performance of solar cells can be further improved if the anisotropic NCs are vertically aligned between the two electrodes to minimize the carrier transport pathways [58]. A detailed discussion is presented in Section 4.

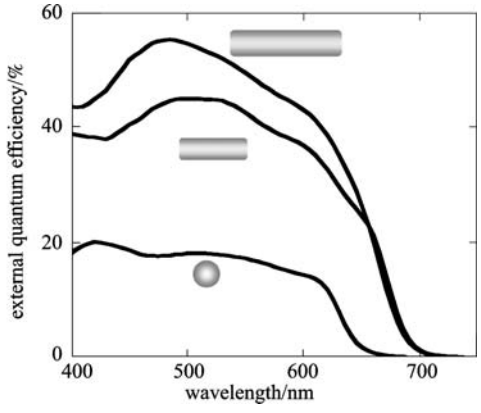

Figure 3 External quantum efficiency of 7 nm-diameter nanorods with the lengths of 7, 30, and 60 nm. Figure was reprinted with permission from Ref. [21].

3 Conjugated polymers

Conjugated polymer is a long chain molecule composed of alternating single and double bonds along the backbone. In CPs, the π electrons are delocalized, hence enable them high mobility compared to the σ electrons. The π electrons shuttle from site to site along a conjugated chain and/or between adjacent polymer chains. The electronic properties of CPs can be described in the context of semiconductor physics, where one-dimensional periodic media is well suited to the basic understanding of an isolated polymer chain [61,62]. The CP used in the nanohybrid solar cells should have an ionization potential lower than 5.2 eV, otherwise the polymers are susceptible to oxidation by O_2 [63]. The commonly used CPs include poly [2-methoxy-5-(2′-ethyl-hexyloxy)-*p*-phenylenevinylene)] (MEH-PPV) and regioregular poly(3-hexylthiophene) (*rr* P3HT). Their chemical structures are shown in Figure 4. The most widely used CP is *rr* P3HT due to its excellent environmental stability, fast hole mobility ($0.1\ cm^2 \cdot V^{-1} \cdot s^{-1}$ in field-effect transistors) and tailorable electrochemical properties [2,64,65]. The CPs are excellent alternatives for crystalline Si due to two reasons: (a) CPs are strong absorbers; and (b) CPs can be deposited on flexible substrates at low cost [16].

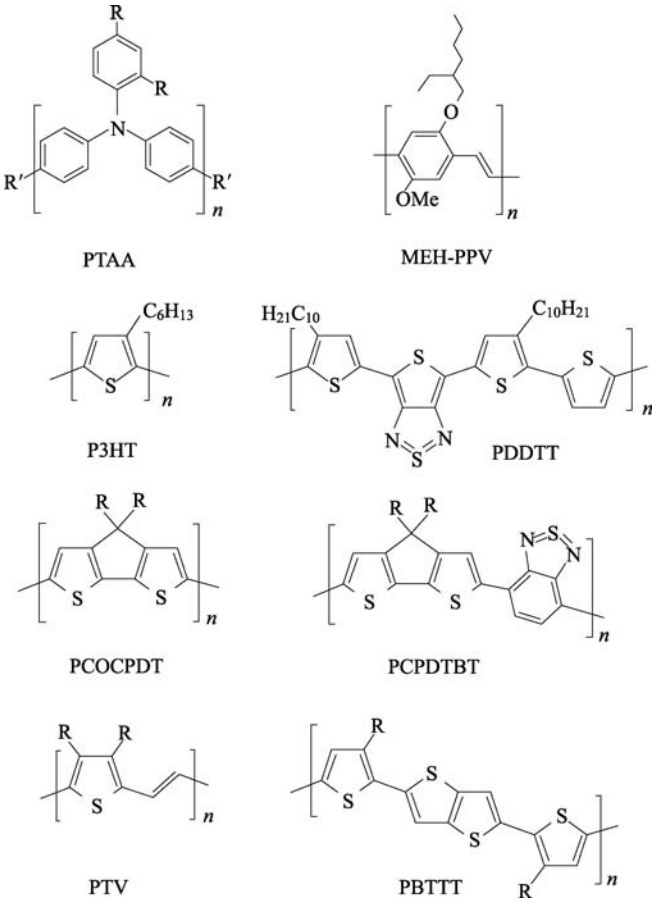

Figure 4 Chemical structures of conjugated polymers commonly used in the CP/NC nanohybrid solar cells. Figure was reprinted with permission from Ref. [2].

Compared to polycrystalline Si with indirect band structure, CPs have direct band structure, which facilitates the excitation of electron without the aid of phonons. Typically, organic semiconductors only have to be 100–500 nm thick in order to absorb most of incident light. In contrast, crystalline Si solar cells should be fabricated around 100 μm thick in order to have the same absorption capability. Taking *rr* P3HT as an example, more than 95% of the incident light is absorbed over the wavelength range of 450–600 nm with the film thickness of only 240 nm (Figure 5) [16]. Consequently, the ability of

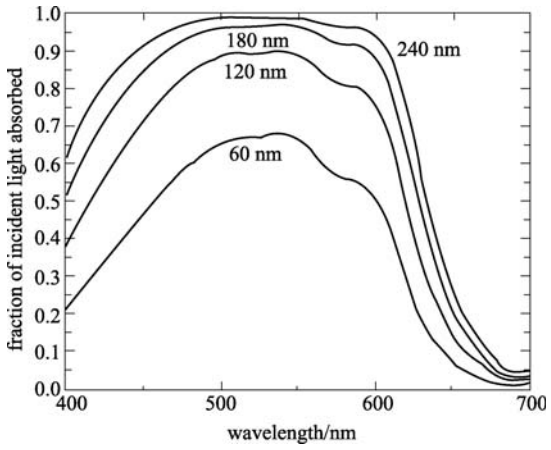

Figure 5 Fraction of incident light absorbed by P3HT film as a function of wavelength for several different film thicknesses. Figure was reprinted with permission from Ref. [16].

CPs to absorb photons at much thinner thickness greatly reduces the fabrication cost of solar cells.

As shown in Figure 4, all commonly used CPs contain side chains that make them soluble in common organic solvents. As a result, well-developed wet-process techniques, e. g., spin coating, dip coating [66], ink-jet printing [67], screen printing [68], and micro molding [69], can be directly employed to fabricate nanohybrid solar cells. All these techniques are performed at mild condition, i.e., at ambient temperature and pressure. Additionally, they are scalable to a large area [16]. Thus, solar cells over large areas can be readily produced in a large scale at the extremely low cost.

Despite a number of advantages, there exist several intrinsic problems for CPs. They need to be tackled in order to obtain high-efficiency CP-based solar cells. First of all, since the band gap of CPs is large and the absorption bandwidth is narrow, only a small fraction of the solar spectrum can be absorbed [16]. Some commonly used CPs, including *rr* P3HT and MEH-PPV, are reported to have the band gap of 3.5–1.9 eV, corresponding the absorption maximum wavelength of 350–650 nm [2]. However, it is around 700 nm for the solar spectrum. This mismatch between the absorption spectra of organic CPs and the solar spectrum offsets the high absorption coefficient of CPs. For example, a 240 nm thick P3HT film can only absorb about 21% of photons from the sun (Figure 5) [16]. To yield high absorption efficiency by better matching with the solar spectrum, the band gap of CPs needs to be largely reduced. It can be realized by increasing the extent of conjugation and the degree of co-planarity [62] as well as by introducing NCs as discussed in Section 2. The second problem is the short diffuse length of excitons in CPs, mainly due to poor carrier mobility. The diffusion length of singlet excitons in most photovoltaic materials is usually 5–10 nm [70], which is much shorter than the absorption depth required for efficient light harvesting. As discussed in Section 1, the excitons generated in CPs have certain lifetime, during which they have to reach the interface and dissociate. If the carrier transport is low, the excitons would recombine or decay before reaching the interface, resulting in a low photocurrent. In the organic semiconductors, the charge transfer is realized by the hopping between localized states rather than by transporting within a continuous chain. Thus the mobility is usually quite low. To improve the overall performance of solar cells, the carrier transport needs to be enhanced. The charge transport can be classified into two categories: the intramolecular charge transport along a conjugated polymer chain and the intermolecular charge transport between adjacent polymer chains. For the former, the charge carrier mobility can be realized by doping, removing or adding electron to the energy band by oxidation or reduction [71–73]. For the latter, the charge carrier mobility can be enhanced by orders of magnitude when the molecular packing is improved. For example, the charge carrier mobility of P3HT is markedly influenced by its regioregularity [74], molecular weight [75–79], and solvent properties [79–81], while the film thickness and annealing condition affect the performance of resulting devices [65]. The intrachain spacing within the thiophene ring plane is unaffected by the variation in regioregularity. However, the interchain spacing perpendicular to the ring plane increases in the case of lower regioregularity, indicating that higher regioregularity should indeed increase the π-π interchain interaction [65]. It is noteworthy that the diffuse length of excitons can also be increased if their lifetime is extended. Compared to singlet excitons, the radiative decay of triplet excitons is dipole forbidden; hence its lifetime is much longer than singlet excitons. Therefore, the overall exciton lifetime can be improved if these singlet excitons can be converted into triplet excitons; this can be realized by doping CPs with transition metal complexes [82].

4 CP/NC composites

Composites of CP/NC are of interest from the standpoint of increased performance relative to either of the non-hybrid counterparts, with many applications envisioned in the areas of solar cells [21,83–85] and LEDs [86–89]. The pioneering work involving composites of organic CPs and inorganic NCs was reported by Greenham et al. in 1996 [83]. They found the photoluminescence (PL) quenching of MEH-PPV after mixing it with 5-nm spherical CdS and CdSe NCs. After removal of the insulating ligand TOPO on the NC surface, the quenching was much stronger. This phenomenon provided evidence for charge transfer because once the exciton was

dissociated, it can no longer decay radiatively to the ground state. They attributed the observed PL quenching to the Forster transfer of the exciton to NC followed by a decay with a radiative efficiency significantly less than that of MEH-PPV [18]. This property (i.e., PL quenching) facilitates the dissociation of exciton at the CP/NC interface and constitutes the base of composites of CP/NC for the use in solar cells. Solar cells fabricated by depositing these composites yielded external quantum efficiency (EQE) of 12% under low intensity light and power conversion efficiency (PCE) of 0.1% subjected to simulated AM 1.5 G irradiation of 100 mW $\cdot$cm^{-2}. Based on the transmission electron microscopy (TEM) images of these composite films, three problems that limit further improvement of device performance are clearly evident. First of all, the NCs tended to aggregate, hence reduced the interfaces of NC/CP. As a result, only few excitons would be able to diffuse to the interface and dissociate, leading to incomplete quenching and thus electron transfer. Second, the loosely connected NC network scattered the electron current and thus less electrons can be collected by electrodes. Finally, the surface of NC was coated with TOPO; these insulating alkyl side chains hindered the efficiency of electron transfer. Over the past decade, different methods have been proposed to overcome these problems. They will be discussed in detail in the following.

4.1 Control of phase separation

As mentioned above, the aggregation of NCs in composites, which is prepared by physically mixing CP and NC, leads to incomplete PL quenching and hence the low electron transfer efficiency. Therefore, a better dispersed NC morphology is favored for the use of composites in solar cells. However, to disperse inorganic NCs at high density within CPs remains challenging, mainly due to the low solubility of NCs in polymers. The dispersion of NC is governed by the solubility parameter (δ), which is proportional to the square root of cohesive energy density and describes the attractive strength between molecules [2]. The solubility of a component in solvent increases as the difference between the solubility parameters of the component and solvent decreases. A solvent that dissolve both NCs and CPs is usually required in order to render good dispersion of NCs,. The solvent is eventually removed in a controllable manner to prevent microphase separation of CPs and NCs by Alivisatos et al.. In their pioneering work, they developed a solvent mixture consisting of one good solvent for NC and another good solvent for CP [21]. Specifically, CdSe nanorods were co-dissolved with P3HT in a mixture of pyridine and chloroform, which are good solvents for CdSe and P3HT, respectively. Subsequent spin-coating process enabled the formation of a uniform film composed of dispersed CdSe nanorods in P3HT. Later on, Alivisatos et al. introduced the tailor-made solvent to achieve less phase separation [90]. By adding the capping ligand to the host solvent, the NCs became more soluble at the expense of the solubility of CP. By varying the concentration of the solvent mixture, phase separation between CP and NC can be tuned from micrometer scale to nanometer scale [90]. Specifically, pyridine passivated CdSe nanorods were first dispersed in the mixed solvent of pyridine/chloroform. Pyridine, which hinders the charge transfer from P3HT to CdSe, was then removed by thermal treatment. As a result, the device performance was greatly improved.

An alternative approach to prevent the microphase separation is to modify the ligands. They were coated on the NC surface to increase their solubility in the CP/NC composites. The phase segregation of NCs is profoundly influenced by their capping ligands [91,92]. Carter et al. studied the ligand effect on the phase segregation of NCs with commonly used ligands, such as butylamine, stearic acid, pyridine, oleic acid, and tributylamine [92]. Butylamine was found to yield the smallest morphological features of NCs within P3HT. It is followed by oleic acid, tributylamine, and stearic acid. A better strategy to promote the complete dispersion of NCs in the CP matrix is to directly graft CPs on the NC surface. This method will be discussed in Section 5.

4.2 Improvement of carrier transport

In addition to phase separation between CP and NC, the performance of the resulting solar cells is also influenced by the efficiency of electron transport. The electrons have to hop between NCs and are often trapped at the end of the NC network. To improve electron collection, it is desirable to form a well-defined pathway, where few traps exist from the CP/NC interface to appropriate electrode. Compared to nanodots or sintered NCs, the use of anisotropic nanorods or tetrapods shows a better performance in solar energy conversion. Such property is due to the fact that the electron has higher mobility along the anisotropic single crystalline nanostructures, where much fewer defects or trap sites exist compared to the nanodot network. Recent efforts in synthesizing anisotropic nanostructures with well defined geometrical shapes [22,33] and assembling them in two and three demensions [93] have further expanded the possibility to develop new strategies for enhanced energy conversion. In this pioneering work, Huynh et al. discovered that electron transport in the film was improved by utilizing slightly elongated NCs that can effectively pack within the film [94]. Later on, they mixed CdSe nanorods with P3HT to fabricate the P3HT/CdSe nanorods hybrid solar cells [21]. Quite intriguingly, the use of these nanorods showed an improved performance and the

PCE of 1.7% was reported. Janssen et al. got a similar observation in the ZnO/poly [2-methoxy-5-(3',7'-dimethyloctyloxy)-1,4-phenylenevinylene] (MDMO-PPV) solar cell [95], where the use of ZnO nanorod led to an improved performance compared to the nanodot counterpart.

As discussed above, one-dimensional nanorods carry several advantages over nanodots. But they tend to lie in the plane of the film, hence is not the optimal arrangement for electron transport. One way to circumvent this problem is to use branched nanostructures, for example tetrapods or hyperbranched NCs. These nanostructures can individually traverse the thickness of the film and have extensions perpendicular to the substrate, thereby providing continuous pathway for transporting electrons. Greenham et al. fabricated composites of CP and branched CdTe NC, which exhibited improved solar cell performance compared to that of previously reported CP/nanorod composites [96]. Under AM 1.5 illumination, the PCE of 1.8% was obtained from a device containing 86 wt% NCs. This result suggested that the increase in PCE is consistent with improved electron transport perpendicular to the plane of the film. Later on, Alivisatos et al. produced ordered CP/NC composites by sequential deposition of CdTe tetrapods and P3HT [97], where the CdTe tetrapods were spontaneously aligned towards the electrodes. The loading and dispersion of tetrapods were easily controlled and characterized. Moreover, the organic and inorganic phases were deposited from their preferred solvents rather than a suboptimal cosolution, therefore the exposure of the NC phase to the top electrode can be controlled. Another way to solve the problem is to pre-form the inorganic phase to maximize the electron mobility, followed by the deposition or infiltration of the CP phase. The pre-formed inorganic phase is typically the fused NC network or vertically oriented anisotropic NC arrays. Kang et al. demonstrated that the vertically aligned CdTe nanorods fabricated by electrodeposition can be used to improve the performance of the poly(3-octylthiophene)/CdTe nanohybrid solar cell by providing a high optical absorption, an efficient charge separation, and a fast electron transport at the poly(3-octylthiophene)/CdTe interface [58]. The PCE of 1.06% was achieved using this method. Later on, vertically aligned CdS nanorod arrays were fabricated on Ti substrates and mixed with MEH-PPV [98]. The PCE of MEH-PPV based solar cell was improved from 0.0012% to 0.60% when combined with these CdS nanoarrays. ZnO columnar arrays were also used in the nanohybrid solar cells prepared by Peiro et al. [99]. These columnar structures provided a direct and ordered path for photogenerated electrons to the collecting electrode [99]. Different CPs (MEH-PPV based polymer and P3HT) were compared in these structures and PCEs of 0.15% and 0.20% were achieved, respectively. Regarding the fused NC network, Heeger et al. infiltrated P3HT into random nanocrystalline TiO_2 networks [100]. Various methods, including heat treatment, surface derivatization, and the use of low molecular weight fraction, were utilized to improve the degree of polymer infiltration. This type of solar cells is similar to the dye sensitized solar cell (DSSC); however, no liquid electrolyte is required in the former one. It is worth noting that the efficiency reported to date is modest because of poor polymer infiltration. More efforts are still needed to be made in this area.

5 CP-NC nanocomposites

Despite various progresses, because CPs and NCs are always in physical contact in the CP/NC composites, it remains difficult to control the detailed morphology and dispersion of NCs within CPs because of the large difference in the solubility of these two components. The interface between CPs and NCs, accomplished by stripping the ligands from the NC surface during film processing [85], is not well controlled, and thus reduced electronic interactions between them. In this context, chemically tethering of NC with CP (i.e., preparing CP-NC nanocomposites with well-controlled interfaces) provides a means to achieve a uniform dispersion of NCs, which carries advantages over cases dominated by NC aggregation. As a result, efficient light induced electronic interactions between CPs and NCs are promoted. Two main synthetic strategies have been successfully performed to yield CP-NC nanocomposites. In the first one, ligand exchange is an essential step either to replace original insulate, small molecules on the NC surface with bifunctional ligands (which contain a second functional group for coupling with conjugated oligomers or polymers) or to directly exchange for the functionalized conjugated oligomers or polymers in a "grafting onto" process. The second strategy utilizes direct grafting of CPs from/onto functionalized NCs in the absence of ligand exchange chemistry [100].

5.1 Ligand exchange

CP-NC nanocomposites can be prepared by exchanging the commonly used, insulate, small molecule-capped NCs with a bifunctional ligand, followed by direct coupling with CPs of interest on the NC surface. The bifunctional ligands consist of the *X-Y-Z* structure, where *X*, *Y*, and *Z* are the functional group for interacting with NCs, the spacer, and the functional group that couples with CPs, respectively [101]. Compared to thiol groups, broadly used for ligand exchange largely due to their commercial availability, organic ligands containing chelating carbodithioate group are excellent binding ligand. They posses higher chemical affinity to NCs by forming strong chelate-type binding with metal atoms, thereby allowing for

the nearly quantitative exchange with original ligand (e.g., TOPO) in very mild conditions and thus improving the resistance of NCs against photo-oxidation as compared to corresponding thiol ligands. Querner et al. quantitatively exchanged initial TOPO ligands on the CdSe surface with 4-formyldithiobenzoic acid. The aniline tetramer was subsequently grafted onto the CdSe surface by a condensation reaction between the terminals as shown in Figure 6 [102,103]. Recently, Zhang et al. used the similar method to graft *rr* P3HT on the CdSe QR surface, yielding P3HT-CdSe QR nanocomposites [104]. Specifically, arylbromide-functionalized CdSe QRs were first synthesized by ligand exchange of pyridine-capped CdSe QRs with *p*-bromobenzyl-di-n-octylphosphine oxide (DOPO-Br). The vinyl-terminated P3HT was then chemically tethered to the CdSe QR surface by Heck coupling with arylbromide moieties. Compared to the composites of P3HT/pyridine-capped CdSe QRs, the P3HT-CdSe QR nanocomposites exhibited an excellent dispersion of QRs in the P3HT matrix. The solid-state PL measurement on the thin film of nanocomposites showed quenching of the emission of P3HT, indicating charge transfer from P3HT to CdSe QRs.

Alternatively, the CP-NC nanocomposites can be achieved by a one-step ligand-exchange reaction with functionalized CPs. In this approach, strong chelating groups (e.g., carbodithioic acid) functionalized CPs or conjugated oligomers (COs) were synthesized first, and were then directly grafted on the NC surface by ligand exchanging with originally capped ligands. For example, Querner et al. synthesized a family of carbodithioic acid functionalized *rr* oligo- and polythiophene as follows [105]. The functionalized thiophene monomer was coupled with oligothiophenes, followed by the oxidative polymerization of the resulting symmetric oligomers. Finally, the carbodithioate moiety was introduced through a post-functionalization reaction, as illustrated in Figure 7. An efficient quenching of PL was observed in the polythiophene-CdSe nanocomposite, revealing a photo-induced charge transfer at the interface of polythiophene and CdSe [105]. Fang et al. grafted CdSe NCs with an amine-containing rod-coil triblock copolymer, poly(2 (dimethylamino)ethylmethacrylate)-poly(fluorene)-poly(2-(dimethyl amino) ethylmethacrylate), by directly ligand exchanging with original insulate TOPO ligands [106]. Recently, Frechet et al. synthesized the amine-terminated P3HT, and used it to partially replace TOPO on the CdSe nanorod surface, leading to a high degree of homogeneity [107]. The partial grafting of P3HT resulted in a better electron transfer, yielding a higher PCE in P3HT-CdSe nanorod solar cells. In addition to linear oligothiophene and polythiophene, conjugated oiligothiophene dendrons were also rationally designed and utilized as electroactive surfactants for capping CdSe QDs [84,108,109].

5.2 Direct grafting

Ligand exchange permits derivatization with a broad range of functional groups on the NC surface. However, it suffers from incomplete surface coverage, although a study on nearly quantitative exchange has been reported recently [103]. As a consequence, the fluorescence emission is quenched due to the aggregations of QDs [110], or oscillates due to adsorption and desorption of surface ligand [111]. Recently, the bifunctional ligand *p*-bromobenzyl-di-octylphosphine oxide (DOPO-Br) was synthesized [112]. It contains a phosphine oxide moiety serving as the anchoring group to the NC surface, and an arylbromide functionality allowing subsequent surface-initiated reaction. DOPO-Br was used as the capping ligand. It replaced TOPO to yield monodispersed

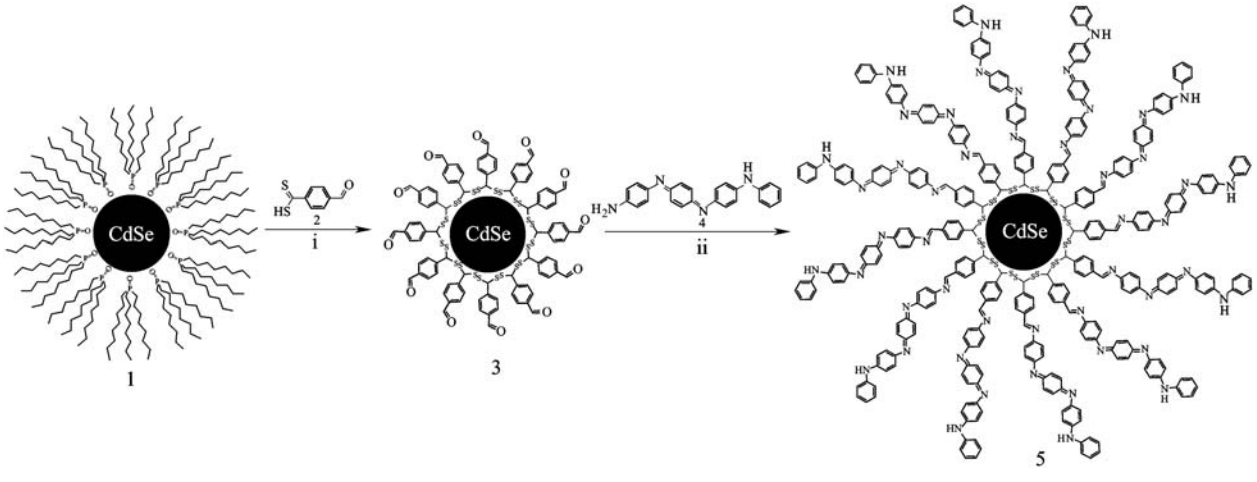

Figure 6 Synthetic pathway for the preparation of aniline tetramer/CdSe nanohybrids. Reprinted with permission from Ref. [103].

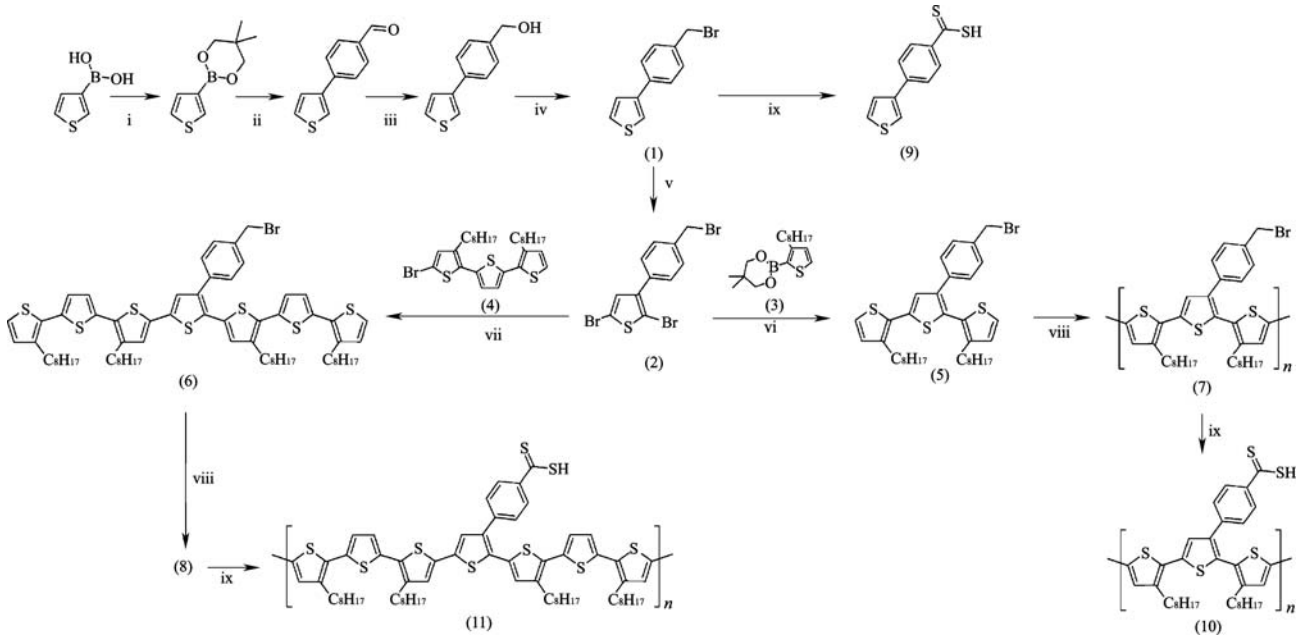

Figure 7 Synthetic pathway for the preparation of a family of carbodithioic acid functionalized regioregular oligo- and polythiophene. Figure was reprinted with permission from Ref. [105].

DOPO-Br functionalized CdSe QDs. With these QDs, Xu et al. grafted relatively longer chain P3HT on the CdSe QD surface via palladium catalyzed Heck coupling, forming P3HT-CdSe QD nanocomposites (Figure 8) [40]. The effective charge transfer from P3HT to CdSe in P3HT-CdSe nanocomposites was confirmed by PL and PL decay measurements. Subsequently, Goodman et al. reported the first study of the behavior of P3HT-CdSe nanocomposites at the air/water interface [113]. Solar cell fabricated from five Langmuir-Blodgett (LB) deposition cycles of the P3HT-CdSe nanocomposites, approximately 30 nm thick, exhibited a relatively high short circuit current, I_{SC}, while maintaining an ultrathin film profile, yielding a PCE of 0.08% [113]. The ultrathin thickness of active layer, ~30 nm, may result in low light absorption and thus low PCE. On the basis of these results, improved photovoltaic performance may be achieved by introducing QDs into CP-QD nanocomposites via forming a better percolation for charge transport, as well as by preparing CP-QR nanocomposites and aligning them in arrays of nanopores that bridge between two electrodes, where the long axis of aligned QRs provide a direct pathway for charge transport.

6 Conclusions and perspective

Recent advances in the organic/inorganic nanohybrids, both prepared by physically mixing CP and NC (i.e., CP/NC composites) and chemically tethering CP with NC (i.e., CP-NC nanocomposites), and their use in solar cells are discussed. These nanohybrid solar cells have low fabrication cost, relatively high photovoltaic performance, and the capability of large-scale production. These advantages make

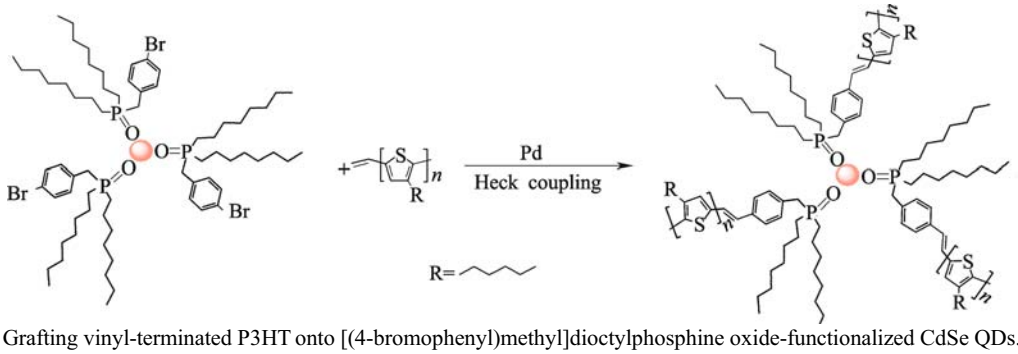

Figure 8 Grafting vinyl-terminated P3HT onto [(4-bromophenyl)methyl]dioctylphosphine oxide-functionalized CdSe QDs. Figure was reprinted with permission from Ref . [40].

them one of the most promising alternatives to challenge conventional Si solar cells and to solve the emergent environmental issue. Further development of solar cells made of the CP/NC composites was limited by the microscopic phase separation, poor carrier collection, and low electronic interaction between two semiconducting components. The strategies to tackle these problems are also reviewed. As newly developed nanohybrid solar cells, the CP-NC nanocomposites carry advantages over the CP/NC composites. More work needs to be done to improve the solar-to-electric energy conversion efficiency.

In spite of progresses over the past decade, the performance of organic/inorganic nanohybrid solar cells is still unsatisfactory. The maximum PCE is only ~5.5% to date. Thus, more strategies need to be introduced to markedly improve PCE, both for CPs and NCs. For example, the double cable morphology, which was proven effective in organic solar cells [114–116], may be helpful for the carrier collection in nanohybrid solar cells. The method for the formation of arrays of anisotropic NCs and subsequent high degree of CP infiltrations should also be further developed to yield improved device performance. Certain small organic molecules, which have higher light absorption efficiency [107], can also be introduced into the organic/inorganic nanohybrids for harvesting more photons.

Acknowledgements We gratefully acknowledge support from the National Science Foundation (NSF-CBET 0824361).

References

1. Schiermeier, Q.; Tollefson, J.; Scully, T.; Witze, A.; Morton, O., *Nature* **2008**, *454*, 816–823
2. Saunders, B. R.; Turner, M. L., *Adv. Colloid Interface Sci*. **2008**, *138*, 1–23
3. Shah, A.; Torres, P.; Tscharner, R.; Wyrsch, N.; Keppner, H., *Science* **1999**, *285*, 692–698
4. Kamat, P. V., *J. Phys. Chem. C* **2008**, *112*, 18737–18753
5. Manna, L.; Scher, E. C.; Alivisatos, A. P., *J. Cluster Sci*. **2002**, *13*, 521–532
6. Peng, X. G., *Adv. Mater*. **2003**, *15*, 459–463
7. Dong, H. X.; Yang, Z.; Yang, W. Y.; Yin, W. Y.; Song, Y. Z.; Yang, H. Q., *Prog. Chem*. **2006**, *18*, 1608–1614
8. Yu, H.; Li, J. B.; Loomis, R. A.; Gibbons, P. C.; Wang, L. W.; Buhro, W. E., *J. Am. Chem. Soc*. **2003**, *125*, 16168–16169
9. Wang, F. D.; Buhro, W. E., *J. Am. Chem. Soc*. **2007**, *129*, 14381–14387
10. Li, L. S.; Alivisatos, A. P., *Adv. Mater*. **2003**, *15*, 408
11. Ghezelbash, A.; Koo, B.; Korgel, B. A., *Nano Lett*. **2006**, *6*, 1832–1836
12. Hu, Z. H.; Fischbein, M. D.; Querner, C.; Drndic, M., *Nano Lett*. **2006**, *6*, 2585–2591
13. Ryan, K. M.; Mastroianni, A.; Stancil, K. A.; Liu, H. T.; Alivisatos, A. P., *Nano Lett*. **2006**, *6*, 1479–1482
14. Kang, C. C.; Lai, C. W.; Peng, H. C.; Shyue, J. J.; Chou, P. T., *Acs Nano* **2008**, *2*, 750–756
15. Querner, C.; Fischbein, M. D.; Heiney, P. A.; Drndic, M., *Adv. Mater*. **2008**, *20*, 2308
16. Coakley, K. M.; McGehee, M. D., *Chemistry of Materials* **2004**, *16*, 4533–4542
17. Jayadevan, K. P.; Tseng, T. Y., *J. Nanosci. Nanotechnol*. **2005**, *5*, 1768–1784
18. Ginger, D. S.; Greenham, N. C., *Phys. Rev. B: Condens. Matter* **1999**, *59*, 10622–10629
19. Campbell, I. H.; Hagler, T. W.; Smith, D. L.; Ferraris, J. P., *Phys. Rev. Lett*. **1996**, *76*, 1900–1903
20. Alvarado, S. F.; Seidler, P. F.; Lidzey, D. G.; Bradley, D. D. C., *Phys. Rev. Lett*. **1998**, *81*, 1082–1085
21. Huynh, W. U.; Dittmer, J. J.; Alivisatos, A. P., *Science* **2002**, *295*, 2425–2427
22. Manna, L.; Scher, E. C.; Alivisatos, A. P., *J. Am. Chem. Soc*. **2000**, *122*, 12700–12706
23. Murray, C. B.; Norris, D. J.; Bawendi, M. G., *J. Am. Chem. Soc*. **1993**, *115*, 8706–8715
24. Chen, M.; Xie, Y.; Lu, J.; Xiong, Y. J.; Zhang, S. Y.; Qian, Y. T.; Liu, X. M., *J. Mater. Chem*. **2002**, *12*, 748–753
25. Pradhan, N.; Xu, H. F.; Peng, X. G., *Nano Lett*. **2006**, *6*, 720–724
26. Yang, J.; Xue, C.; Yu, S. H.; Zeng, J. H.; Qian, Y. T., *Angew. Chem. Int. Ed*. **2002**, *41*, 4697–4700
27. Zhan, J. H.; Yang, X. G.; Wang, D. W.; Li, S. D.; Xie, Y.; Xia, Y.; Qian, Y. T., *Adv. Mater*. **2000**, *12*, 1348–1351
28. Duan, X. F.; Lieber, C. M., *Adv. Mater*. **2000**, *12*, 298–302
29. Gudiksen, M. S.; Lieber, C. M., *J. Am. Chem. Soc*. **2000**, *122*, 8801–8802
30. Duan, X. F.; Huang, Y.; Cui, Y.; Wang, J. F.; Lieber, C. M., *Nature* **2001**, *409*, 66–69
31. Fan, H. J.; Werner, P.; Zacharias, M., *Small* **2006**, *2*, 700–717
32. Peng, Z. A.; Peng, X. G., *J. Am. Chem. Soc*. **2001**, *123*, 183–184
33. Peng, Z. A.; Peng, X. G., *J. Am. Chem. Soc*. **2002**, *124*, 3343–3353
34. Hu, J. T.; Li, L. S.; Yang, W. D.; Manna, L.; Wang, L. W.; Alivisatos, A. P., *Science* **2001**, *292*, 2060–2063
35. Medintz, I. L.; Uyeda, H. T.; Goldman, E. R.; Mattoussi, H., *Nat. Mater*. **2005**, *4*, 435–446
36. Gaponik, N.; Talapin, D. V.; Rogach, A. L.; Hoppe, K.; Shevchenko, E. V.; Kornowski, A.; Eychmuller, A.; Weller, H., *J. Phys. Chem. B* **2002**, *106*, 7177–7185
37. Zhang, H.; Wang, D.; Mohwald, H., *Angew. Chem. Int. Ed*. **2006**, *45*, 6244–6244
38. Donega, C. D.; Liljeroth, P.; Vanmaekelbergh, D., *Small* **2005**, *1*, 1152–1162
39. Wang, Y.; Herron, N., *J. Phys. Chem*. **1991**, *95*, 525–532
40. Xu, J.; Wang, J.; Mitchell, M.; Mukherjee, P.; Jeffries-EL, M.; Petrich, J. W.; Lin, Z. Q., *J. Am. Chem. Soc*. **2007**, *129*, 12828–

12833
41. Skaff, H.; Sill, K.; Emrick, T., *J. Am. Chem. Soc*. **2004**, *126*, 11322–11325
42. Schaller, R. D.; Agranovich, V. M.; Klimov, V. I., *Nat. Phys*. **2005**, *1*, 189–194
43. Schaller, R. D.; Klimov, V. I., *Phys. Rev. Lett*. **2004**, 92
44. Schaller, R. D.; Sykora, M.; Pietryga, J. M.; Klimov, V. I., *Nano Lett*. **2006**, *6*, 424–429
45. Luque, A.; Marti, A.; Nozik, A. J., *MRS Bull*. **2007**, *32*, 236–241
46. Luther, J. M.; Beard, M. C.; Song, Q.; Law, M.; Ellingson, R. J.; Nozik, A. J., *Nano Lett*. **2007**, *7*, 1779–1784
47. Murphy, J. E.; Beard, M. C.; Norman, A. G.; Ahrenkiel, S. P.; Johnson, J. C.; Yu, P. R.; Micic, O. I.; Ellingson, R. J.; et al., *J. Am. Chem. Soc*. **2006**, *128*, 3241–3247
48. Beard, M. C.; Knutsen, K. P.; Yu, P. R.; Luther, J. M.; Song, Q.; Metzger, W. K.; Ellingson, R. J.; Nozik, A. J., *Nano Lett*. **2007**, *7*, 2506–2512
49. Ellingson, R. J.; Beard, M. C.; Johnson, J. C.; Yu, P. R.; Micic, O. I.; Nozik, A. J.; Shabaev, A.; Efros, A. L., *Nano Lett*. **2005**, *5*, 865–871
50. Pijpers, J. J. H.; Hendry, E.; Milder, M. T. W.; Fanciulli, R.; Savolainen, J.; Herek, J. L.; Vanmaekelbergh, D.; Ruhman, S.; et al., *J. Phys. Chem. C* **2007**, *111*, 4146–4152
51. Schaller, R. D.; Sykora, M.; Jeong, S.; Klimov, V. I., *J. Phys. Chem. B* **2006**, *110*, 25332–25338
52. Shabaev, A.; Efros, A. L.; Nozik, A. J., *Nano Lett*. **2006**, *6*, 2856–2863
53. Trinh, M. T.; Houtepen, A. J.; Schins, J. M.; Hanrath, T.; Piris, J.; Knulst, W.; Goossens, A. P. L. M.; Siebbeles, L. D. A., *Nano Lett*. **2008**, *8*, 1713–1718
54. Franceschetti, A.; Zhang, Y., *Phys. Rev. Lett*. **2008**, 100
55. Guyot–Sionnest, P., *Nat. Mater*. **2005**, *4*, 653–654
56. Schaller, R. D.; Petruska, M. A.; Klimov, V. I., *Appl. Phys. Lett*. **2005**, 87
57. Fu, A. H.; Gu, W. W.; Boussert, B.; Koski, K.; Gerion, D.; Manna, L.; Le Gros, M.; Larabell, C. A.; et al., *Nano Lett*. **2007**, *7*, 179–182
58. Kang, Y. M.; Park, N. G.; Kim, D., *Appl. Phys. Lett*. **2005**, 86
59. Zhang, Q. L.; Gupta, S.; Emrick, T.; Russell, T. P., *J. Am. Chem. Soc*. **2006**, *128*, 3898–3899
60. Li, L. S.; Hu, J. T.; Yang, W. D.; Alivisatos, A. P., *Nano Lett*. **2001**, *1*, 349–351
61. Agrawal, G. P.; Cojan, C.; Flytzanis, C., *Phys. Rev. Lett*. **1977**, *38*, 711–715
62. Nunzi, J. M., *Comptes Rendus Physique* **2002**, *3*, 523–542
63. Kim, Y. G.; Thompson, B. C.; Ananthakrishnan, N.; Padmanaban, G.; Ramakrishnan, S.; Reynolds, J. R., *J. Mater. Res*. **2005**, *20*, 3188–3198
64. Coakley, K. M.; Liu, Y. X.; McGehee, M. D.; Frindell, K. L.; Stucky, G. D., *Adv. Funct. Mater*. **2003**, *13*, 301–306
65. Kim, Y.; Cook, S.; Tuladhar, S. M.; Choulis, S. A.; Nelson, J.; Durrant, J. R.; Bradley, D. D. C.; Giles, M.; et al., *Nat. Mater*. **2006**, *5*, 197–203
66. Wang, G. M.; Swensen, J.; Moses, D.; Heeger, A. J., *J. Appl. Phys*. **2003**, *93*, 6137–6141
67. Hebner, T. R.; Wu, C. C.; Marcy, D.; Lu, M. H.; Sturm, J. C., *Appl. Phys. Lett*. **1998**, *72*, 519–521
68. Pschenitzka, F.; Sturm, J. C., *Appl. Phys. Lett*. **1999**, *74*, 1913–1915
69. Rogers, J. A.; Bao, Z. N.; Raju, V. R., *Appl. Phys. Lett*. **1998**, *72*, 2716–2718
70. Halls, J. J. M.; Pichler, K.; Friend, R. H.; Moratti, S. C.; Holmes, A. B., *Appl. Phys. Lett*. **1996**, *68*, 3120–3122
71. Pei, Q. B.; Yu, G.; Zhang, C.; Yang, Y.; Heeger, A. J., *Science* **1995**, *269*, 1086–1088
72. Yamamoto, T.; Morita, A.; Miyazaki, Y.; Maruyama, T.; Wakayama, H.; Zhou, Z.; Nakamura, Y.; Kanbara, T.; .et al., *Macromolecules* **1992**, *25*, 1214–1223
73. Gross, M.; Muller, D. C.; Nothofer, H. G.; Scherf, U.; Neher, D.; Brauchle, C.; Meerholz, K., *Nature* **2000**, *405*, 661–665
74. Sirringhaus, H.; Brown, P. J.; Friend, R. H.; Nielsen, M. M.; Bechgaard, K.; Langeveld-Voss, B. M. W.; Spiering, A. J. H.; Janssen, R. A. J. et al., *Nature* **1999**, *401*, 685–688
75. Zhang, R.; Li, B.; Iovu, M. C.; Jeffries-EL, M.; Sauve, G.; Cooper, J.; Jia, S. J.; Tristram-Nagle, S.; et al., *J. Am. Chem. Soc*. **2006**, *128*, 3480–3481
76. Kline, R. J.; McGehee, M. D.; Kadnikova, E. N.; Liu, J. S.; Frechet, J. M. J., *Adv. Mater*. **2003**, *15*, 1519
77. Zen, A.; Pflaum, J.; Hirschmann, S.; Zhuang, W.; Jaiser, F.; Asawapirom, U.; Rabe, J. P.; Scherf, U.; Neher, D., *Adv. Funct. Mater*. **2004**, *14*, 757–764
78. Kline, R. J.; Mcgehee, M. D.; Toney, M. F., *Nat. Mater*. **2006**, *5*, 222–228
79. Kline, R. J.; McGehee, M. D.; Kadnikova, E. N.; Liu, J. S.; Frechet, J. M. J.; Toney, M. F., *Macromolecules* **2005**, *38*, 3312–3319
80. Chang, J. F.; Sun, B. Q.; Breiby, D. W.; Nielsen, M. M.; Solling, T. I.; Giles, M.; McCulloch, I.; Sirringhaus, H., *Chem. Mater*. **2004**, *16*, 4772–4776
81. Bao, Z.; Lovinger, A. J.; Dodabalapur, A., *Appl. Phys. Lett*. **1996**, *69*, 3066–3068
82. Yang, C. M.; Wu, C. H.; Liao, H. H.; Lai, K. Y.; Cheng, H. P.; Horng, S. F.; Meng, H. F.; Shy, J. T., *Appl. Phys. Lett*. **2007**, 90
83. Greenham, N. C.; Peng, X. G.; Alivisatos, A. P., *Phys. Rev. B: Condens. Matter* **1996**, *54*, 17628–17637
84. Milliron, D. J.; Alivisatos, A. P.; Pitois, C.; Edder, C.; Frechet, J. M. J., *Adv. Mater*. **2003**, *15*, 58
85. Milliron, D. J.; Gur, I.; Alivisatos, A. P., *MRS Bull*. **2005**, *30*, 41–44
86. Odoi, M. Y.; Hammer, N. I.; Sill, K.; Emrick, T.; Barnes, M. D., *J. Am. Chem. Soc*. **2006**, *128*, 3506–3507
87. Colvin, V. L.; Schlamp, M. C.; Alivisatos, A. P., *Nature* **1994**, *370*, 354–357
88. Coe, S.; Woo, W. K.; Bawendi, M.; Bulovic, V., *Nature* **2002**, *420*, 800–803
89. Lee, J.; Sundar, V. C.; Heine, J. R.; Bawendi, M. G.; Jensen, K. F., *Adv. Mater*. **2000**, *12*, 1102

90. Huynh, W. U.; Dittmer, J. J.; Libby, W. C.; Whiting, G. L.; Alivisatos, A. P., *Adv. Funct. Mater*. **2003**, *13*, 73–79
91. Aldakov, D.; Chandezon, F.; De Bettignies, R.; Firon, M.; Reiss, P.; Pron, A., *Eur. Phys. J. Appl. Phys*. **2006**, *36*, 261–265
92. Olson, J. D.; Gray, G. P.; Carter, S. A., *Sol. Energy Mater. Sol. Cells* **2009**, *93*, 519–523
93. Schierhorn, M.; Boettcher, S. W.; Ivanovskaya, A.; Norvell, E.; Sherman, J. B.; Stucky, G. D.; Moskovits, M., *J. Phys. Chem. C* **2008**, *112*, 8516–8520
94. Huynh, W. U.; Peng, X. G.; Alivisatos, A. P., *Adv. Mater*. **1999**, *11*, 923
95. Beek, W. J. E.; Wienk, M. M.; Kemerink, M.; Yang, X. N.; Janssen, R. A. J., *J. Phys. Chem. B* **2005**, *109*, 9505–9516
96. Sun, B. Q.; Marx, E.; Greenham, N. C., *Nano Lett*. **2003**, *3*, 961–963
97. Gur, I.; Fromer, N. A.; Alivisatos, A. P., *J. Phys. Chem. B* **2006**, *110*, 25543–25546
98. Kang, Y.; Kim, D., *Sol. Energy Mater. Sol. Cells* **2006**, *90*, 166–174
99. Peiro, A. M.; Ravirajan, P.; Govender, K.; Boyle, D. S.; O'Brien, P.; Bradley, D. D. C.; Nelson, J.; Durrant, J. R., *J. Mater. Chem*. **2006**, *16*, 2088–2096
100. Bartholomew, G. P.; Heeger, A. J., *Adv. Funct. Mater*. **2005**, *15*, 677–682
101. Lin, Z. Q., *Chem. Eur. J*. **2008**, *14*, 6294–6301
102. Querner, C.; Reiss, P.; Bleuse, J.; Pron, A., *J. Am. Chem. Soc*. **2004**, *126*, 11574–11582
103. Querner, C.; Reiss, P.; Sadki, S.; Zagorska, M.; Pron, A., *PCCP* **2005**, *7*, 3204–3209
104. Zhang, Q. L.; Russell, T. P.; Emrick, T., *Chem. Mater*. **2007**, *19*, 3712–3716
105. Querner, C.; Benedetto, A.; Demadrille, R.; Rannou, P.; Reiss, P., *Chem. Mater*. **2006**, *18*, 4817–4826
106. Fang, C.; Qi, X. Y.; Fan, Q. L.; Wang, L. H.; Huang, W., *Nanotechnology* **2007**, *18*, 35704
107. Liu, J. S.; Tanaka, T.; Sivula, K.; Alivisatos, A. P.; Frechet, J. M. J., *J. Am. Chem. Soc*. **2004**, *126*, 6550–6551
108. Locklin, J.; Patton, D.; Deng, S. X.; Baba, A.; Millan, M.; Advincula, R. C., *Chem. Mater*. **2004**, *16*, 5187–5193
109. Advincula, R. C., *Dalton Trans*. **2006**, 2778–2784.
110. Kalyuzhny, G.; Murray, R. W., *J. Phys. Chem. B* **2005**, *109*, 7012–7021
111. Komoto, A.; Maenosono, S.; Yamaguchi, Y., *Langmuir* **2004**, *20*, 8916–8923
112. Goodman, M. D.; Xu, J.; Wang, J.; Lin, Z. Q., *Chem. Mater*. **2009**, *21*, 934–938
113. Tan, Z.; Hou, J. H.; He, Y. J.; Zhou, E. J.; Yang, C. H.; Li, Y. F., *Macromolecules* **2007**, *40*, 1868–1873
114. Spanggaard, H.; Krebs, F. C., *Sol. Energy Mater. Sol. Cells* **2004**, *83*, 125–146
115. Possamai, G.; Maggini, M.; Menna, E.; Scorrano, G.; Franco, L.; Ruzzi, M.; Corvaja, C.; Ridolfi, G.; Samori, P.; Geri, A.; Camaioni, N., *Appl. Phys. A* **2004**, *79*, 51–58
116. Sun, X. B.; Zhou, Y. H.; Wu, W. C.; Liu, Y. Q.; Tian, W. J.; Yu, G.; Qiu, W. F.; Chen, S. Y.; Zhu, D. B., *J. Phys. Chem. B* **2006**, *110*, 7702–7707